

Mars 2020 Rover Laser Power Supply Thermomechanical Analysis

Juan Cepeda-Rizo and David Tuman
Jet Propulsion Laboratory,
NASA / Californian Institute of Technology
Pasadena, CA, 91109-8099, USA
juan.cepeda-rizo@jpl.nasa.gov

Abstract—Operation of the Laser Power Supply (LPS) module provides the dual challenge of high power dissipation, and the need for strict dielectric isolation, while needing to survive in an environment on Mars that will see a chilly night-time temperature of -123°C , and to a daytime instrument environment in excess of 50°C . Additionally, power restrictions prevent the use of survival heating during the night. The harsh mechanical vibration environment of launch and landing provides an additional challenge to reliability. A multi-physics simulation was created that took into account temperature property variations, as well as solving the transient analysis that also included rapid variation in power-pulsing during the operation of the laser. The steady state analysis employed a more traditional finite element based analysis, but with provisions for Mars gas convection and thermal radiation.

Keywords—Laser; Mars; Rover; 2020; Power Electronics

I. INTRODUCTION (HEADING 1)

The Laser Power Supply (LPS) is an essential part of the SHERLOC instrument (Scanning Habitable Environments with Raman & Luminescence for Organics and Chemicals), slated for NASA's Mars 2020 rover (Figure 1) [1]. SHERLOC's LPS provides the power to the laser that will shine a tiny dot of ultraviolet laser light at a target producing a distinctive fluorescence, or glow, from molecules that contain rings of carbon atom that offer clues to whether evidence of past life has been preserved. The laser will also induce Raman scattering, which can identify certain minerals, including ones formed from evaporation of salty water, and organic compounds. This dual use enables powerful analysis of many different compounds on the identical spot.

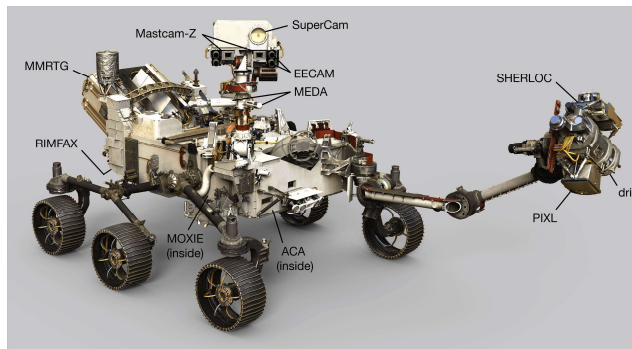


Figure 1. Mars 2020 Rover showing SHERLOC on the turret assembly.

II. DESIGN CONSIDERATION: THERMAL AND ELECTRICAL ISOLATION

The LPS was designed to provide the most effective through-board thermal conduction path while providing electrical isolation to prevent corona discharge. A thermal model of the complete Laser Power Supply (LPS) chassis assembly including both Main Printed Wiring Assembly (PWA) and capacitor banks PWAs, was created using Solidworks Simulation finite element code and composed of 60,267 nodes and 29,771 elements.

The Main Printed Wiring Board (PWB) was attached to the chassis using ten perimeter M2 screws having a thermal resistance of $3^{\circ}\text{C}/\text{W}$ each. The PWB is wet-mounted to the chassis with Nusil 2946 thermal bonding adhesive around the entire perimeter. The chassis thermal attachment to the 70°C sink is through a bracket and a flexure at each end. A total dissipation of 15.2 W was applied to main board spread across five devices, while the capacitor banks were treated as passive. Mars atmosphere gas conduction and radiation at 70°C were included in the model. Thermal planes were estimated across the entire main board with focus placed on careful spreading estimation underneath the high power MOSFET devices M3 and M4.

A transient analysis was performed of M3 and M4 to assure that a duty cycle of 50% of the peak power estimate was adequate. The TX2 inductor device was assumed to conduct heat away by means of an M2 screw to the chassis, while the rest of the devices conducted heat through solder pads into the main PWB.

III. MATERIALS

A. Printed Wiring Board (PWB) Model

For the PWB laminate thermal conductivity values, orthotropic values were used derived by the board stack up for each PWB [2]. The effective thermal conductivities both in-plane of the PWB (in the XY plane of the board), and in the out-plane transverse direction (Z-direction) are as follows:

$$k_{in-plane} = \frac{\sum_{i=1}^N \eta_i k_i t_i}{\sum_{i=1}^N t_i}$$

$$k_{out-plane} = \frac{\sum_{i=1}^N t_i}{\sum_{i=1}^N \frac{t_i}{\eta_i k_i}}$$

Where k_i = thermal conductivity of the i th layer,
 t_i = thickness of i th layer,
 η_i = % copper of the i th signal, power, or ground layer
(correction factor)

B. Thermal Results

Thermal Results

Figure 1 shows the results of the thermal analysis, with a hottest temperature of 112.4 °C measured underneath M4.

Figure 1. Thermal gradient of Main PWB showing min and max temperatures.

IV. TRANSIENT THERMAL ANALYSIS

A transient analysis was performed of the M3 and M4 MOSFETs to assure that a duty cycle of 50% of the peak power estimate was adequate [3]. The laser is to operate with 40 usec pulses with a total time-on of 10 seconds, and time-off of 10 seconds. The pulses are assumed to be on for 40 usec, and off for 40 usec. So essentially there are two cycles to consider, a 10 seconds off/on main cycle,

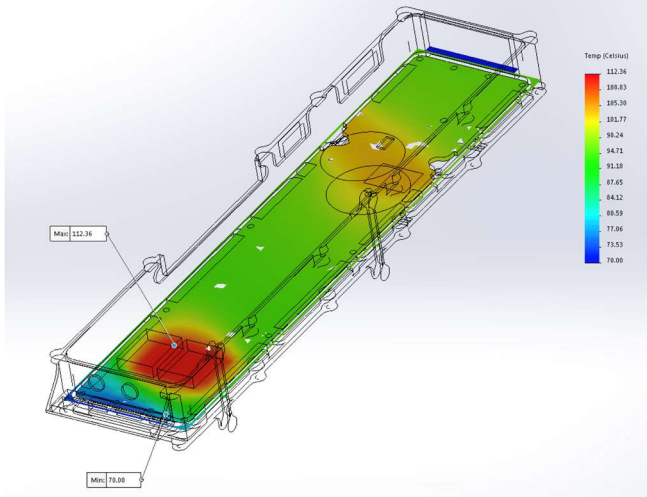


Figure 1. Steady state maximum temperatures of MOSFETs shown as 112.36°C for a boundary temperature of 70°C .

and a 40 usec on/off sub-cycle. It is clear that the duty cycle from an energy standpoint was 50% (e.g. the power is on only 50% of the time), but the intent is to see how the temperature varies as a function of time to entertain reducing on/off cycles as a means of reducing overall temperature. Figure 2 shows the 10 seconds on, 10 seconds off power cycling as well as the 40 usec pulses. Figure 3 shows the transient temperature across 100 seconds.

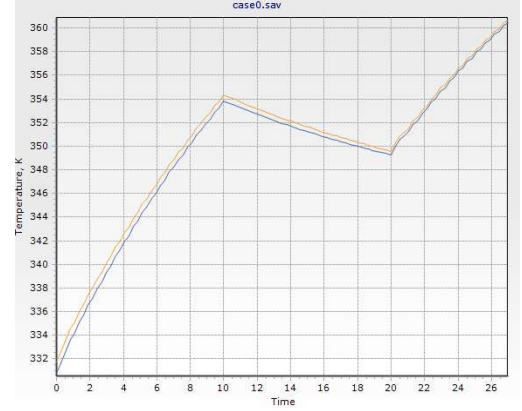


Figure 2. Thermal transient of Main PWB showing min and max temperatures for 10 seconds on, 10 seconds off, and 7 seconds on.

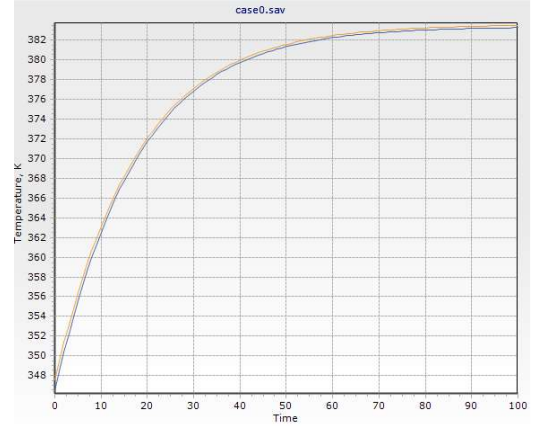


Figure 3. Thermal transient of Main PWB showing min and max temperatures for continuous power across 100 seconds.

A. Steinburg Fatigue Analysis

A structural analysis of the LPS assembly was performed using the required environment 7.9 Grms random vibration spectrum for the Atlas V launch vehicle [5]. The spectrum is applied in the worst-case direction with damping at 2%. The PWA deflection response was found to be within the guidelines of reference 6 (Steinburg)[6] for a vibration fatigue life of 20 million cycles, which is 8 hours of vibration at the fundamental PWB vibration frequency of 783 Hz (see Figure 4), the next mode is shown in Figure 5.

Aluminum chassis and cover margin against yielding was 6.47. Total model mass is 1,024 grams.

The lowest frequency vibration mode was the capacitor bank PWA at 783 Hz. Highest RMS von Mises stress in the chassis (Figure 6) was 46 MPa at the base of one of the PWA supports; peak stress was taken as the 3-sigma value, or 138 MPa. Cover stresses were less than 50% of this. PWB flexure allowance per reference 6 is .0107" for the Main PWA, and .0148" for the capacitor bank PWAs compared to the modeled 3-sigma PWB flexure of .0017" (Figure 7), and .0007" (Figure 8), respectively.

The first mode of the LPS assembly was 176 Hz (Figure 9) and occurred at the capacitor bank structure, which was made of Polyetherimide (ULTEM™). The associated stress with the deflection was very small compared with the tensile strength.

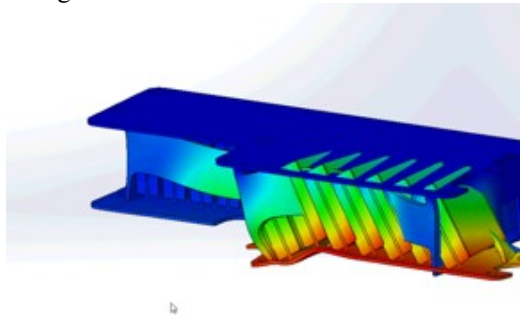


Figure 4. 5th Mode of capacitor bank PWA was 783 Hz.

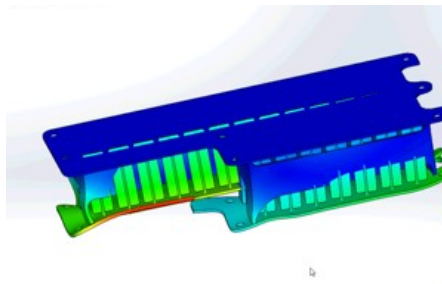


Figure 5. 6th Mode capacitor bank PWA was 1067 Hz

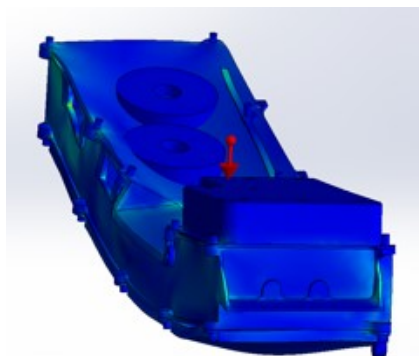


Figure 6. Maximum Chassis Stress is 4.6E+07 N/m².

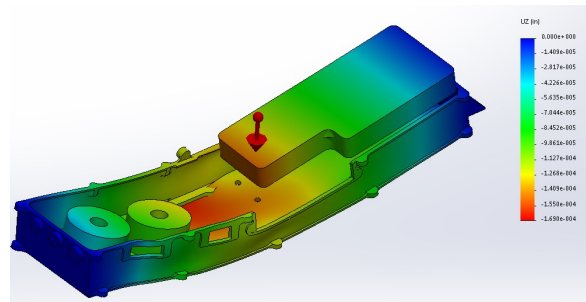


Figure 7. Main PWB modeled maximum deflection is .0017"

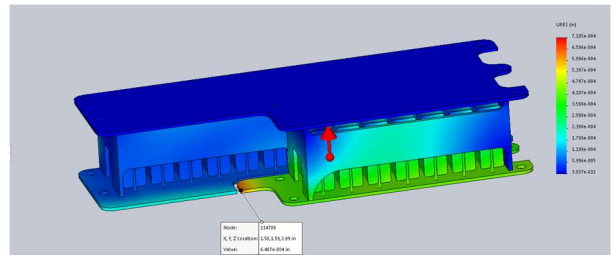


Figure 8. Cap Bank PWB modeled maximum deflection is .0007"

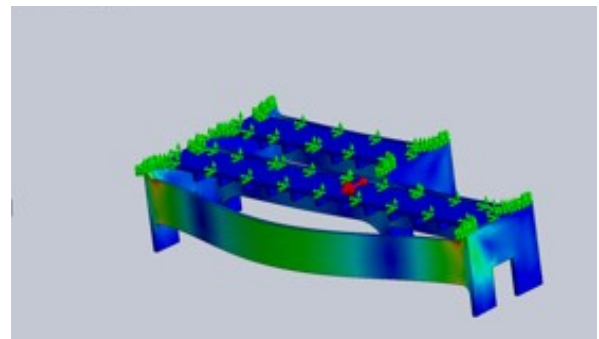


Figure 9. 1st mode of LPS model occurs at the capacitor bank structure, is 176 Hz. The stress associated with the deflection was negligible.

B. Chassis Fasteners

Figure 6 and Table 1 shows the results of the modeled slipping and gapping analysis results for the chassis fasteners. Table 2 shows the axial force value of each M2 fastener in the model. 3-sigma gapping load at the highest loaded M2 mounting fastener is 130 N. The margin was large compared to the expected M2 reduced preload of 832.5 N, or FS of +6.4 per JPL guidelines for fasteners with non-lubricated threads into an insert. 3-sigma slipping load was 61 N. The margin was large compared to the slipping capability of 166.5 N, or FS of +2.73. Positive margins are acceptable.

Table 1. Gapping and Slipping Factor of Safety Results.

Fastener	Axial Force (N)	Shear 1	Shear 2	3 σ Gapping Load (N)	3 σ Slipping Load (N)	Reduced Load	Slipping Capability	Red. Load/Gap. Load	Slip
MAX	43.33	1.6	11.2	130	61	832.5	166.5	6.4	

MI2x.7 Max Preload Table 14 JPL D-51878 = 1250 N (282.81 lbf)
Minimum Preload: 77% of Original = 962.5 N (217.7 lbf)
Coefficient of friction - mating assemblies = 0.2

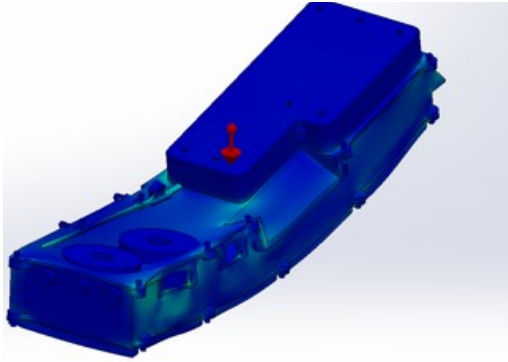


Figure 7. Chassis and M2 screws stress analysis

Table 2. Modeled Screw Stresses

LPS M2 Bottom Cover	A286 Stress	LPS M2 Top Cover	A286 Stress
Node	Value (N/m ²)	Node	Value (N/m ²)
48526	1.09E+07	60276	5.89E+05
1297	3.98E+06	61387	3.57E+05
49359	1.47E+06	61342	7.12E+05
49090	2.03E+06	50494	2.80E+06
48718	2.27E+06	50501	3.29E+06
48813	3.10E+06	83635	3.56E+06
44921	1.31E+06	83734	1.42E+06
48850	2.99E+06	60035	8.57E+06
49130	1.15E+07	60007	6.43E+06
48385	9.56E+06	50540	3.20E+06
48994	4.34E+06	59911	3.89E+06

the generous amount of feed through area for wire routing from top to bottom of the main PWA, well below the necessary requirement, where V is volume, and A is feed through area [4]. A conservative 1 psi was assumed as the pressure differential based on Figure 8 guideline. The result shown in Figure 9 was a maximum stress at the chassis of 1.04E+08 N/m² for an ultimate tensile strength of 3.1E+08 N/m² for Al 6061-T6, renders a factor of safety of 2.98, which exceeds the recommended factor safety of 2.0.

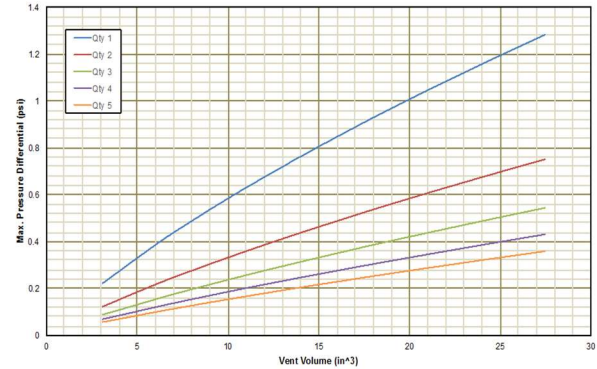


Figure 8. Vent volume vs. pressure differential

D. Conclusion

The analysis showed that the Main PWA as well as the capacitor bank PWAs had no issues when subjected to the random vibration environment against the environment requirements. A venting analysis of the LPS assembly passed the guidelines as well.

E. Acknowledgement

We would like to thank Rufus Simon for the design of the board electronics, and Paul Eryan for leading the manufacturing effort.

The research was carried out at the Jet Propulsion Laboratory, California Institute of Technology, under a contract with the National Aeronautics and Space Administration.

REFERENCES

- [1] L. Beegle, et. al., "Scanning habitable environments with Raman & luminescence for organics & chemicals," IEEE Aerospace 2015, 2015, Page(s):1 - 11
- [2] B. Joiner, "evaluation of Thermal Characterization Techniques," Proc. of IEPS Convergence, 1994, pp. 460-467.
- [3] T.D. Panczak, S. Ring, Thermal Desktop Manual, version.6, 17 May 2017, chapter 20, pp. 65-70.
- [4] P. Kurowski, "Engineering Analysis Using Solidworks Simulation 2017," SDC Publication, March 15, 2017.
- [5] R. Dillman, "Planned Assembly, Integration, and Testing of a 6M Hiad Orbital Entry Vehicle.," 14th International Planetary Probe Workshop, June 12 2017
- [6] D. Steinberg, Vibration Analysis for Electronic Equipment, 3rd edition, John Wiley & Son, 2000

Table 3. Steinburg Fatigue Analysis Results

Steinburg PCB Deflection Analysis									
max PCB deflection 3sigma		PCB Length, in		compt length		PCB t		Constant	
	Z, inches	Z, mm	B	L	h	C	r	placement	PSD, G
M3 & IM4 LCCC, LPS Main		0.0107	0.272	9.100	0.787	0.094	2.250	1.000	
LPS Caps PWBs		0.0148	0.376	9.843	1.000	0.098	1.500	1.000	
Expected Main PWB Deflection (3sigma) from FEM		0.0017	0.04318						
	Factor of Safety		6.30						

C. Venting Analysis

A venting analysis was conducted on the LPS mechanical model. The LPS was measure to have a total of 3.5 E+04 in³ of air space inside the module. The space above and below the main PWA were assumed to be one space due to